BULETINUL INSTITUTULUI POLITEHNIC DIN IAŞI
Publicat de
Universitatea Tehnică „Gheorghe Asachi” din Iaşi
Volumul 63 (67), Numărul 1, 2017
Secţia
CHIMIE şi INGINERIE CHIMICĂ

MODELLING THE FREE RADICAL POLYMERIZATION OF STYRENE USING ARTIFICIAL NEURAL NETWORKS

BY

LUCIANA GHIBA, ELENA-NICULINA DRĂGOI and SILVIA CURTEANU[*]

“Gheorghe Asachi” Technical University of Iaşi,
Faculty of Chemical Engineering and Environmental Protection

Received: March 22, 2017
Accepted for publication: March 29, 2017

Abstract. In this work, the modeling of free radical polymerization of styrene is performed using two approaches: phenomenological and empirical. In the last case, artificial neural networks are used, applying two working strategies. First, a single model with three outputs (monomer conversion, numerical molecular weight and gravimetrical molecular weights) based on time, temperature and initial concentration of the initiator (model inputs) was determined. Due to the unacceptable performance results for the molecular weights, a second strategy is developed, modelling each output, separately, as function of the three inputs. Different artificial neural network topologies were tested, the two hidden layer networks performing the best for all the outputs.

Keywords: styrene; modelling; prediction; artificial neural networks.

1. Introduction

Polystyrene is one of the most well-known and intensively studied polymers and is predominantly obtained by a radical mechanism under the action of heat, with or without initiator.

---

[*] Corresponding author; *e-mail*: scurtean@tuiasi.ro

The block polymerization of styrene has the ability to produce polystyrene of superior optical clarity and outstanding electrical properties. Mass polymerization allows the production of blocks, bars and transparent plates, without pressing, which is important for the manufacture of parts for the high-frequency electrochemical industry. On the other hand, bulk polymerization of styrene has a series of disadvantages due to its high viscosity and reduced thermal conductivity of the formed polymer. Since the polymerization process is strongly exothermic and the polystyrene is a bad heat conductor, inside the block, local overheating zones are formed which lead to a different rate of polymerization and, therefore, to a different degree of polymerization in the various portions of the block.

In this work, free radical polymerization of styrene, conducted in mass, is approached by simulation. The mathematical modelling takes into account the usual stages of radical polymerization: initiation, propagation, termination by recombination and chain transfer to monomer.

The initiation of the process can be realized chemically, but at higher temperatures (above 100°C) one should also consider the thermal initiation.

A major feature of the homogeneous free radical polymerization is the important increase of the mass reaction viscosity with monomer conversion. As a consequence, diffusional effects (gel and glass effects) appear, producing a deviation from normal kinetic and significant changes of mass and heat transfer.

In the literature, there are many approaches concerning the modeling of styrene polymerization, but their domain is limited because the great operational difficulties represented by the complex reaction kinetics, inherent process nonlinearities and the continuous demand for running these reactors at varying operating conditions needed to produce different polymer grades. The usual practice for operating polymerization reactors is to optimize the reactor temperature profile since the end use properties of the product polymer depend highly on temperature. For instance, Hosen *et al*. (2011) implemented and used experimentally a neural network-model predictive control (NN-MPC) algorithm to control the temperature of a polystyrene (PS) batch reactors. The obtained predictions are then introduced in a numerical optimization procedure which attempts to minimize a specified cost function to calculate a suitable control signal at each sample instant. It was concluded that the NN-MPC performance is superior to the conventional PID controller, especially during process startup.

Hossen and Hussain (2012) developed an optimization procedure for a polystyrene batch reactor based on a hybrid model – a first principle-Neural network model used to design the controller which implements the optimum temperature profile.

The prediction interval (PI)-based modelling techniques are introduced and applied to capture the nonlinear dynamics of a polystyrene batch reactor system (Hosen *et al.*, 2014). Simple neural networks are designed for modeling, but their parameters are adjusted using simulated annealing optimization technique with the goal to minimize the PI-based cost function.

Soft sensing technology is usually applied for determining polymer molecular weight distribution (MWD) because of the lack of the on-line measurement instrument. The orthogonal polynomials combined with neural networks, *i.e*. soft sensing model, was used to simulate the real-time changes of MWD, using, as measurable variables, average molecular weight and low-order moment statistics (Ding *et al*., 2015).

The main goal of this paper is to elaborate and check a complete model for bulk or suspension polymerization of styrene. A comparative approach is presented, developing a phenomenological model which include diffusional effects and neural networks for modeling the monomer conversion and polymer molecular weights as function of initiator concentration, time and reaction temperature. It was proved that both models are satisfactory, emphasizing their advantages and disadvantages and, also, conditions in which their use is recommended.

2. Modelling Methodologies

2.1. Phenomenological Model

The styrene bulk polymerization in the presence of a single initiator can be represented by the following reactions:

$$\text{Initiation} \qquad \begin{cases} I \xrightarrow{k_d} 2R^{**} \\ R^* + M \xrightarrow{k_i} P_1^* \\ 3M \xrightarrow{k_{iterm}} P_1^* + P_2^* \end{cases} \tag{1}$$

$$\text{Propagation} \qquad P_n^* + M \xrightarrow{k_p} P_{n+1}^* \tag{2}$$

$$\text{Chain transfer to monomer} \qquad P_n^* + M \xrightarrow{k_{tm}} D_n + P_1^* \tag{3}$$

$$\text{Termination by recombination} \qquad P_n^* + P_m^* \xrightarrow{k_{tc}} D_n + D_m \tag{4}$$

In the above kinetic diagram, I is the initiator, R^* – primary radical, M – monomer, P_n^* – macro-radical with n monomer units, D_n – dead chain with n monomer units, k_d, k_i, k_{iterm}, k_p, k_{tm}, k_{tc} – rate constants for decomposition of initiator, chemical initiation, thermal initiation, propagation, chain transfer to monomer and termination by recombination, respectively.

From the kinetic diagram one can write the balance equations for the monomer and initiator concentrations (M, I) and for the distribution moments of macro-radicals (λ_i) and of dead polymer (μ_i, $i = 0,1,2$).

$$\frac{dI}{dt} = -k_d I - \frac{\varepsilon I}{1+\varepsilon x}\left(k_{iterm} M_0^2 \left(\frac{1-x}{1+\varepsilon x}\right)^2 + k_p \lambda_0 + k_{tm} \lambda_0\right)(1-x) \tag{5}$$

$$\frac{dx}{dt} = \left(k_{iterm} M_0^2 \left(\frac{1-x}{1+\varepsilon x}\right)^2 + k_p \lambda_0 + k_{tm} \lambda_0\right)(1-x) \tag{6}$$

$$\begin{aligned} \frac{d\lambda_0}{dt} &= 2 f k_d I + 2 k_{iterm} M_0^3 \left(\frac{1-x}{1+\varepsilon x}\right)^3 - k_{tc} \lambda_0^2 - \\ &- \frac{\varepsilon \lambda_0}{1+\varepsilon x}\left(k_{iterm} M_0^2 \left(\frac{1-x}{1+\varepsilon x}\right)^2 + k_p \lambda_0 + k_{tm} \lambda_0\right)(1-x) \end{aligned} \tag{7}$$

$$\begin{aligned} \frac{d\lambda_1}{dt} &= 2 f k_d I + 3 k_{iterm} M_0^3 \left(\frac{1-x}{1+\varepsilon x}\right)^3 + k_p M_0 \left(\frac{1-x}{1+\varepsilon x}\right)\lambda_0 - k_{tc} \lambda_0 \lambda_1 - \\ &- \lambda_1 \varepsilon \frac{1-x}{1+\varepsilon x}\left(k_{iterm} M_0^2 \left(\frac{1-x}{1+\varepsilon x}\right)^2 + k_p \lambda_0 + k_{tm} \lambda_0\right) - k_{tm} M_0 \left(\frac{1-x}{1+\varepsilon x}\right)(\lambda_1 - \lambda_0) \end{aligned} \tag{8}$$

$$\begin{aligned} \frac{d\lambda_2}{dt} &= 2 f k_d I + 5 k_{iterm} M_0^3 \left(\frac{1-x}{1+\varepsilon x}\right)^3 + k_p M_0 \left(\frac{1-x}{1+\varepsilon x}\right)(2\lambda_1 + \lambda_0) - k_{tc} \lambda_0 \lambda_2 - \\ &- \lambda_2 \varepsilon \frac{1-x}{1+\varepsilon x}\left(k_{iterm} M_0^2 \left(\frac{1-x}{1+\varepsilon x}\right)^2 + k_p \lambda_0 + k_{tm} \lambda_0\right) - k_{tm} M_0 \left(\frac{1-x}{1+\varepsilon x}\right)(\lambda_2 - \lambda_0) \end{aligned} \tag{9}$$

$$\begin{aligned} \frac{d\mu_0}{dt} &= \frac{1}{2} k_{tc} \lambda_0^2 - \mu_0 \varepsilon \frac{1-x}{1+\varepsilon x}\left(k_{iterm} M_0^2 \left(\frac{1-x}{1+\varepsilon x}\right)^2 + k_p \lambda_0 + k_{tm} \lambda_0\right) + \\ &+ k_{tm} M_0 \left(\frac{1-x}{1+\varepsilon x}\right)\lambda_0 \end{aligned} \tag{10}$$

$$\begin{aligned} \frac{d\mu_1}{dt} &= k_{tc} \lambda_0 \lambda_1 - \mu_1 \varepsilon \frac{1-x}{1+\varepsilon x}\left(k_{iterm} M_0^2 \left(\frac{1-x}{1+\varepsilon x}\right)^2 + k_p \lambda_0 + k_{tm} \lambda_0\right) + \\ &+ k_{tm} M_0 \left(\frac{1-x}{1+\varepsilon x}\right)\lambda_1 \end{aligned} \tag{11}$$

$$\begin{aligned}\frac{d\mu_2}{dt} &= k_{tc}\lambda_0\lambda_2 - \mu_2\varepsilon\frac{1-x}{1+\varepsilon x}\left(k_{iterm}M_0^2\left(\frac{1-x}{1+\varepsilon x}\right)^2 + k_p\lambda_0 + k_{tm}\lambda_0\right) + \\ &+ k_{tm}M_0\left(\frac{1-x}{1+\varepsilon x}\right)\lambda_2 + k_{tc}\lambda_1^2\end{aligned} \tag{12}$$

As the polymerization proceeds, the constants k_{tc} and k_p decrease due to the diffusional constraints, gel and glass effects, respectively Chiu *et al*. (1983) proposed for these constants the following models:

$$\frac{1}{k_t} = \frac{1}{k_{t0}} + \theta_t\frac{\lambda_0}{exp\left[\dfrac{2.303(1-x)}{A+B(1-x)}\right]} \tag{13}$$

$$\frac{1}{k_p} = \frac{1}{k_{p0}} + \theta_p\frac{\lambda_0}{exp\left[\dfrac{2.303(1-x)}{A+B(1-x)}\right]} \tag{14}$$

$$\theta_t = \frac{\theta_t^0}{I_0}exp\left(\frac{E_{\theta_t}}{RT}\right) \tag{15}$$

$$\theta_p = \theta_p^0\, exp\left(\frac{E_{\theta_p}}{RT}\right) \tag{16}$$

$$A = C_1 - C_2(T - T_{gp})^2 \tag{17}$$

where: $E_{\theta_t}, E_{\theta_p}$ are activation energies for θ_t and θ_p; T – polymerization temperature and T_{gp} – glass transition temperature of the polymer; θ_t, θ_p – characteristic migration times; θ_t^0, θ_p^0 – pre-exponential factors for θ_{tc} and θ_p, C_1, C_2 – constants, k_{t0}, k_{p0} – termination and propagation rate constants in the absence of gel and glass effects.

For the rate constant of chain transfer to monomer, a similar decrease to that of propagation rate constant was proposed (Chiu *et al.*, 1983) because both reactions involve the same diffusion mechanism – the monomer molecules migrating toward the growing macro-radicals.

$$k_{tm} = k_{tm0}\frac{k_p}{k_{p0}} \tag{18}$$

Simulations were conducted in Matlab, using an own software program.

2.2. Neural Network Modelling

An alternative to classical modeling is represented by an empirical method - artificial neural network (ANN).

Neural networks, through their efficient representative – feed-forward neural network – are mostly used because of their simplicity, flexible structure, good quality of the predictions, and the capability of acting as universal approximator.

Particularly for polymerization processes, characterized by complex reaction mechanisms and models, difficult to develop and solve, neural network modeling becomes a viable option, given that it does not require extensive knowledge of process phenomenology. Only input-output data, representative in number and value range, are required to achieve satisfactory results.

In this work, three input variables were considered: initiator concentration, I_0, with values in the range 20-60 mol/m^3, reaction temperature, T, in the domain 70-120°C and polymerization time, t, 0-5000 min. Each simulation had specific intervals for the above parameters, depending of the values for temperature and initiator amount, so that complete curves for conversion and molecular be obtained. The outputs of the neural network models were: monomer conversion, x, numerical molecular weight, M_n and gravimetrical molecular weight, M_w. Two types of modeling were conducted in order to obtain better results – MLP(3:x:3) and MLP(3:x:1) were developed, meaning multilayer perceptron with three outputs, attempting to model all the three variables simultaneously and networks with a single output variable, when separate models were determined for each of the considered variables (x, M_n, M_w). In both cases, neural networks with one or two intermediate layers and different number of hidden neurons were designed.

From simulations, a large database is obtained with more than 10 000 data, making difficult their handling. A specific procedure was added in a Matlab software where a variable step is considered, with small values during the gel effects and higher in the other intervals, aiming the precise reproduction of the effects controlled by diffusion. This resulted in a dataset of about 4000 values which means a reasonable and sufficient number of data.

Fig. 1 presents the two ways of neural network modeling applied to free radical polymerization of styrene.

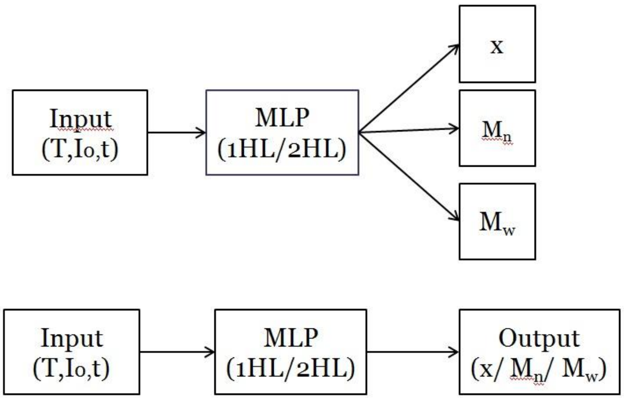

Fig. 1 – Neural network modeling procedures.

NeuroSolutions, a dedicated software, is used for developing and testing feed-forward neural networks of different structures (number of hidden layers and neurons).

3. Results and Discussion

3.1. Phenomenological Modelling Results

Using a Matlab software program, many simulations were made under different reaction conditions, represented by temperature and amount of the initiators in the reaction mixture. A single initiator was used: benzoylperoxide (POB).

The properties of the chemical initiator, as well as other constants used in simulation of styrene polymerization, are given in Table 1.

Table 1
Numerical Values for Kinetics of Styrene Polymerization

$k_d^0(POB) = 1.2\times10^{13}\ \mathrm{s^{-1}}$

$k_{p0}^0 = 1.051\times10^4\ \mathrm{m^3/(mol\ s)}$

$k_{tm0}^0 = 2.31\times10^3\ \mathrm{m^3/(mol\ s)}$

$k_{tc0}^0 = 1.26\times10^6\ \mathrm{m^3/(mol\ s)}$

$k_{iterm}^0 = 2.19\times10\ \mathrm{(m^3)^2/(mol^2\ s)}$

$E_{iterm} = 1.56\times10^5\ \mathrm{J/mol}$

$E_d\ (POB) = 1.2\times10^5\ \mathrm{J/mol}$

$E_p = 2.958\times10^4\ \mathrm{J/mol}$

$E_{tm} = 5.275\times10^4\ \mathrm{J/mol}$

Table 1

Continuation

E_{tc} = 7.04 × 10^3 J/mol

$k_d = k_d^0 \exp\left(-E_d/(RT)\right)$

$k_{p0} = k_{p0}^0 \exp\left(-E_p/(RT)\right)$

$k_{tm0} = k_{tm0}^0 \exp\left(-E_{tm}/(RT)\right)$

$k_{tc0} = k_{tc0}^0 \exp\left(-E_{tc}/(RT)\right)$

$k_{iterm} = k_{iterm}^0 \exp\left(-E_{iterm}/(RT)\right)$

$f\,(POB)$ = 0.6

C_1 = 0.091678; C_2 = 1.142 × 10^{-5}

T_{gp} = 373.16 K

θ_p^0 = 7.4053 × 10^{-3} s; $E_{\theta p}$ = 4.634 × 10^4 J/mol

θ_{tc}^0 = 0.53598 × 10^{-8} (mol s)/m^3

$E_{\theta tc}$ = 9.5722 × 10^4 J/mol

ρ_m = 924 – 0.918 × T [°C]

ρ_p = 1084.8 – 0.685 × T [°C]

$\varepsilon = (\rho_m - \rho_p)/\rho_p$

The meaning of all notations in Table 1 is given in Section 2.1. In addition, k_{tc0} and k_{p0} represent propagation and termination rate constants in the absence of glass and gel effects; k_d^0, k_{iterm0}^0, k_{p0}^0, k_{tc0}^0, k_{tm0}^0 are frequency factors; E_d, E_{iterm}, E_p, E_{tc}, E_{tm} – activation energies; ρ_m, ρ_p – monomer and polymer densities.

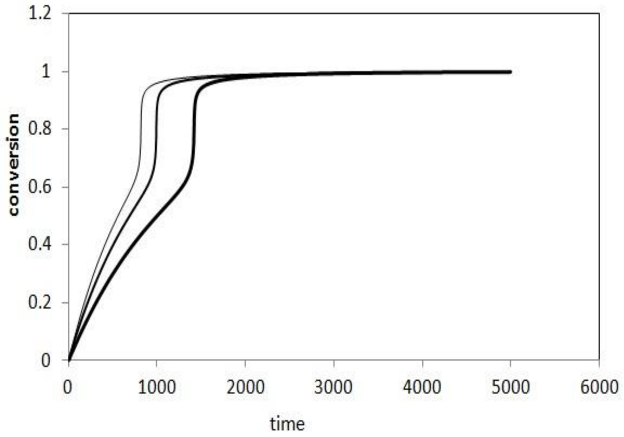

Fig. 2 – The variation in time of monomer conversion obtained using POB as initiator when the temperature is 70ºC.

Figs. 2-4 illustrate the variation in time of monomer conversion, numerical and gravimetrical molecular weights obtained using POB as initiator when the temperature is 70ºC, for different values of the initial concentration of the initiator: 20, 40, 60 mol/m^3, respectively.

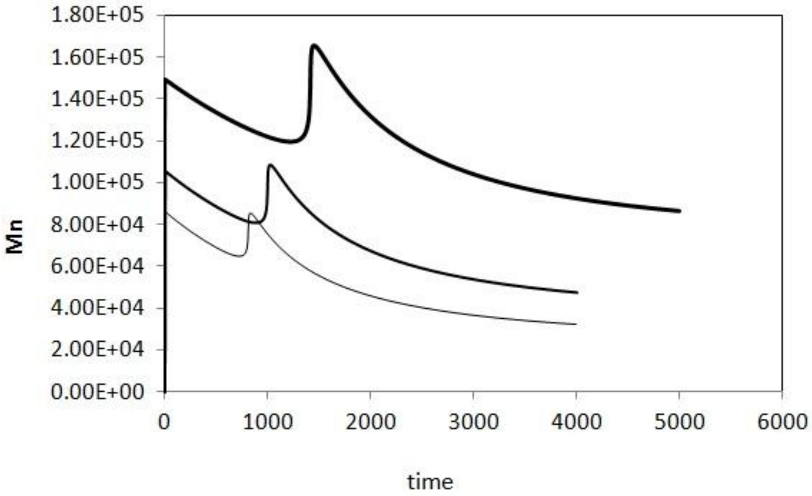

Fig. 3 – The variation in time of numerical molecular weight obtained using POB as initiator when the temperature is 70ºC.

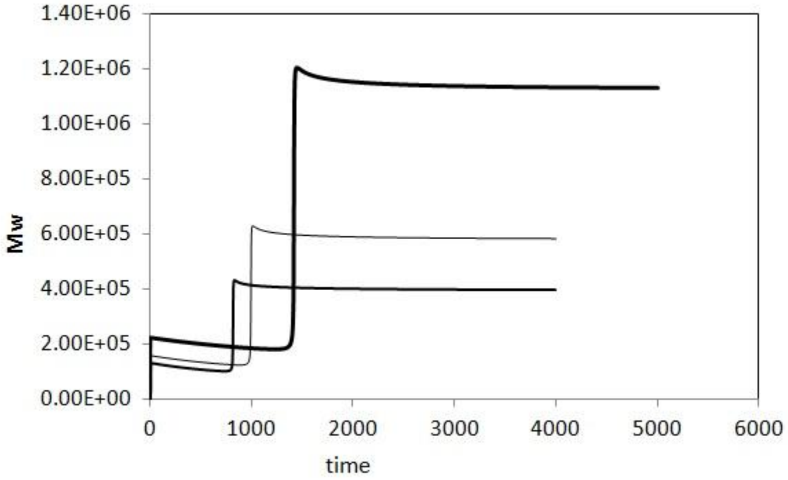

Fig. 4 – The variation in time of gravimetrical molecular weight obtained using POB as initiator when the temperature is 70ºC.

A sudden increase of conversion or molecular mass corresponds to the gel effect, appearing at different combination of temperature and initiator concentration. This is a difficult part to model in the free radical polymerization.

Figs. 5-7 show the variation in time of x, M_n and M_w obtained with POB as initiator when the temperature is 120ºC, for different values of the initial concentration of the initiator: 40, 50, 60 mol/m^3, respectively.

Some interesting observations can be made from the simulation at 120°C, with chemical decomposition of POB and thermal decomposition of the monomer. As can be seen in Fig. 5, the polymerization with POB gives a monomer conversion with a maximum value of 60% because of rapid consumption of the free radicals (dead – end polymerization). For this, a solution would be to add a second slow initiator, for instance tertbutylperbenzoate (TBPB) (Curteanu and Bulacovschi, 2003).

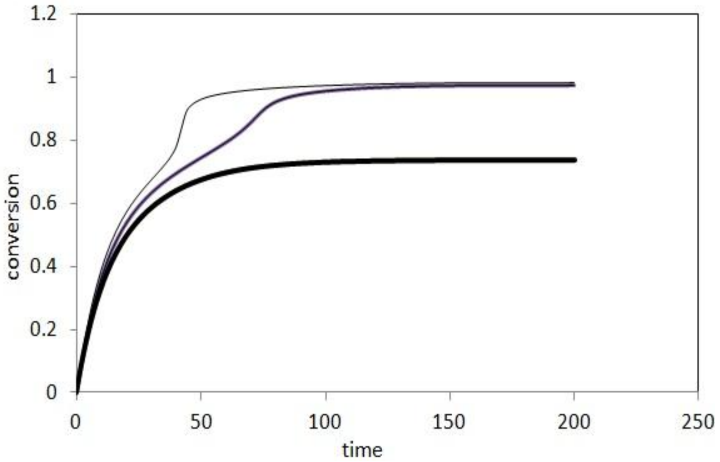

Fig. 5 – The variation in time of monomer conversion obtained using POB as initiator when the temperature is 120ºC.

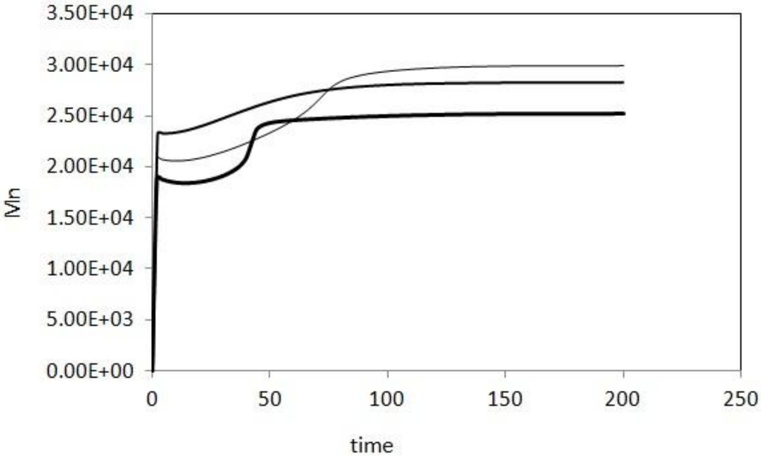

Fig. 6 – The variation in time of numerical molecular weight obtained using POB as initiator when the temperature is 120ºC.

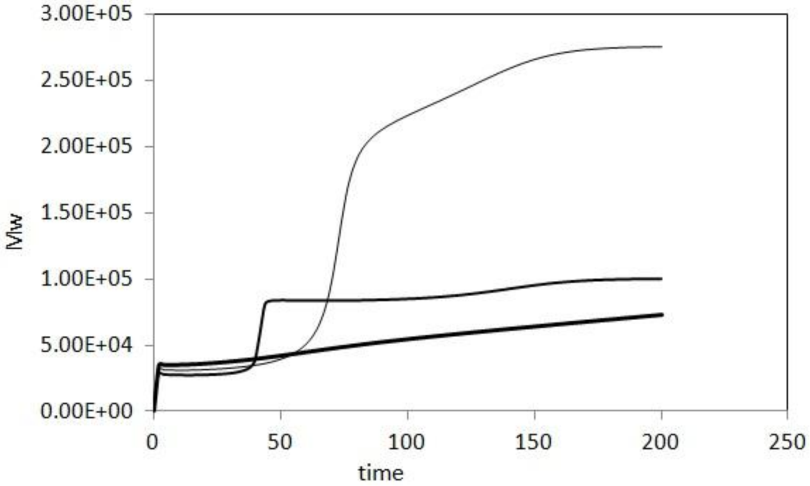

Fig. 7 – The variation in time of gravimetrical molecular weight obtained using POB as initiator when the temperature is 120ºC.

3.2. Neural Network Modelling Results

After the simulation data was gathered and processed, a series of neural network topologies were developed, trained and tested using *NeuroSolution* software. Initially, a structure combining all three parameters (x, M_n, M_w) was considered. However, although general good mean squared error (*MSE*) and correlation (r) values were obtained, when performing a point by point comparison between the simulation data and the ANN predictions, it was observed that for M_n and M_w, relatively high differences are present (Figs. 8 and 9).

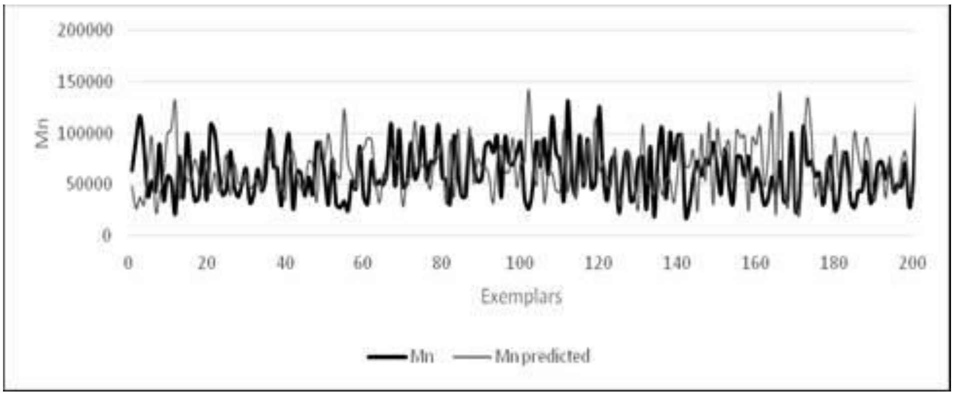

Fig. 8 – Comparison between simulation data and ANN predicted for some points from the testing set in case of the M_n output.

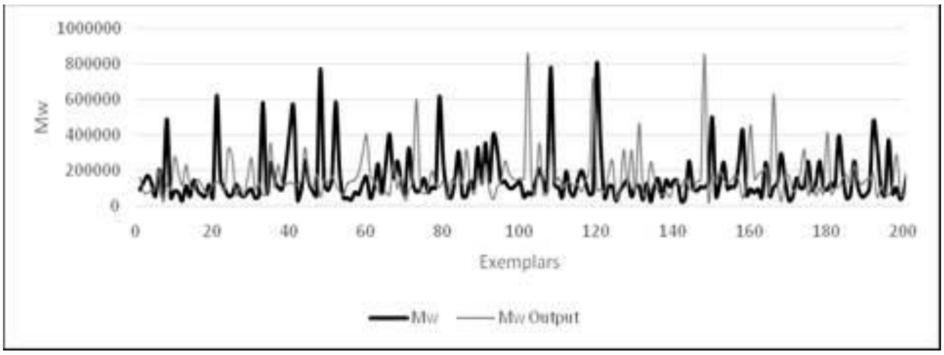

Fig. 9 – Comparison between simulation data and ANN predicted for some points from the testing set in case of the M_w output.

Consequently, the next step consisted in determining individual models for each output. In this case, multiple structures were tested (Table 2).

Table 2

Topologies Tested for Each Output

x		M_n		M_w	
Topology	r	Topology	r	Topology	r
4:50:1	0.9834	4:50:1	0.9756	4:30:1	0.8748
4:40:1	0.9834	4:40:1	0.9760	4:40:1	0.8698
4:30:1	**0.9847**	**4:30:1**	**0.9798**	**4:50:1**	**0.8997**
4:20:1	0.9827	4:20:1	0.9743	4:60:1	0.8797
4:25:1	0.9830	4:25:1	0.9784	4:55:1	0.8857
4:40:25:1	0.9929	**4:40:25:1**	**0.9878**	4:40:25:1	0.9362
4:30:10:1	**0.9932**	4:30:10:1	0.9821	4:30:15:1	0.9260
4:25:10:1	0.9855	4:25:10:1	0.9851	**4:40:20:1**	**0.9434**
4:30:5:1	0.9909	4:30:5:1	0.9784	4:40:15:1	0.9255
4:25:15:1	0.9869	4:25:15:1	0.9802	4:25:10:1	0.8954
4:30:15:1	0.9880	4:30:15:1	0.9756	–	–

In Table 2, the bold, grey coloring indicates the best solutions (highest *r*) obtained with one and two hidden layers. A point by point comparison between simulated and ANN predictions for the three outputs is presented in Figs. 10-12 for a series of production data (data that was not included in the training/testing phases).

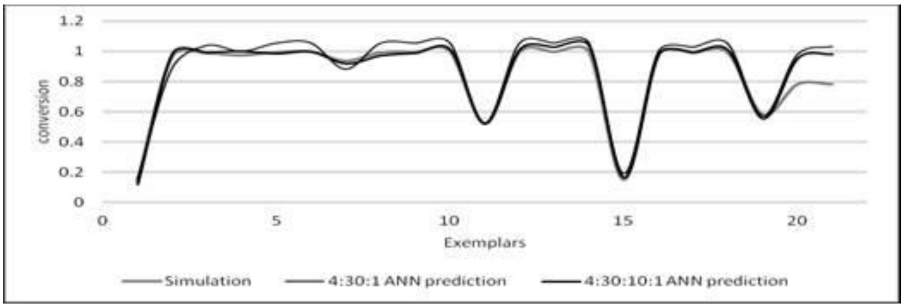

Fig. 10 – Comparison between simulation data and ANN predicted for some points from the production set in case of the x output.

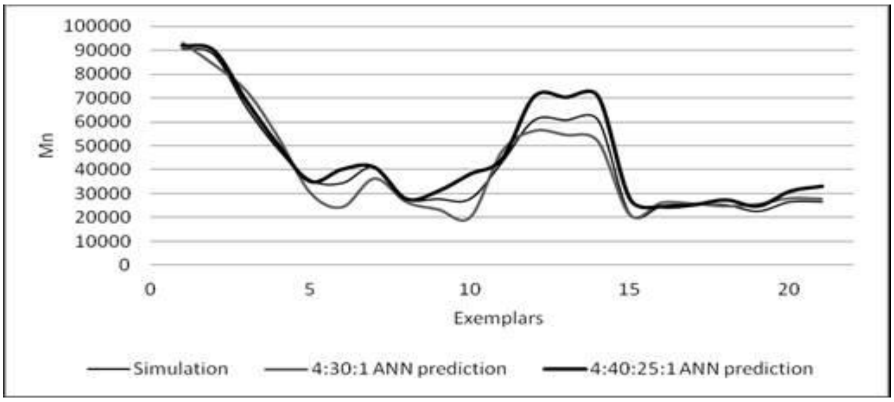

Fig. 11 – Comparison between simulation data and ANN predicted for some points from the production set in case of the M_n output.

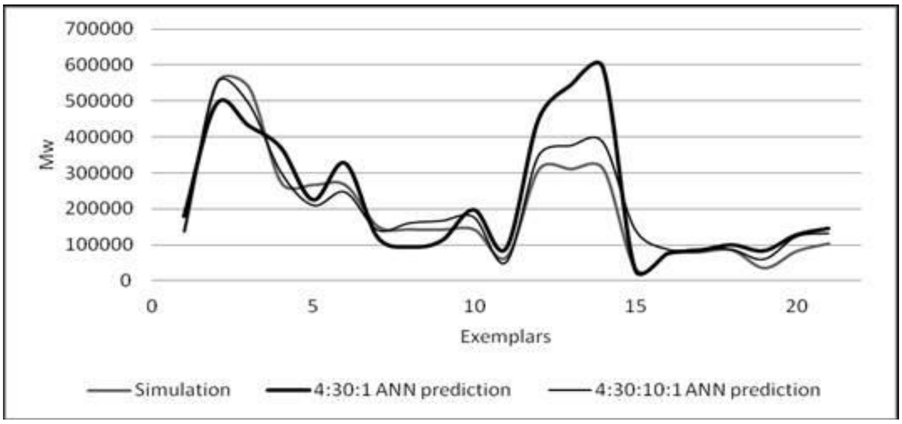

Fig. 12 – Comparison between simulation data and ANN predicted for some points from the production set in case of the M_w output.

As it can be observed from Figs. 10-12, the predictions obtained with the two hidden layer ANN models are closer to the simulation data, fact which indicates that they better capture the process dynamic and can be used to replace the simulations in various conditions.

4. Conclusions

The bulk/suspension polymerization of styrene was simulated employing a model which considers the chemical and thermal initiation, gel and glass effects. For reactions carried out below 100°C, only the decomposition of initiators is considered, and over 100°C, both initiation mechanisms, decomposition of initiators and monomer decomposition.

The theoretical approach of this paper emphasizes the influence of some parameters on polymerization process: amount of initiators, time and temperature. Many and important information can be obtained carrying out the simulations under a large domain of different reaction conditions. Thus, the necessary number of experiments becomes smaller because they are chosen depending on simulation results.

The artificial neural network employed in this work focused on two distinct approaches: modelling all the outputs using a single model and individual models for each output. The first approach tested (a single model for all outputs) provided unacceptable results from the performance point of view, fact which lead to the application of the second approach, where different configurations were tested: with one and two hidden layers and different number of intermediate neurons. For all the three outputs, the ANN with two hidden layers proved to be the best, with a correlation in the range of 0.94-0.99.

A future study will continue this approach with styrene polymerization under nonisothermal and semi-discontinuous reaction conditions, in addition with model improvement through hybridization (the combination of phenomenological with empirical models).

REFERENCES

Chiu W.Y, Carratt G.M., Soong D.S., *A Computer Model for the Gel Effect in Free-Radical Polymerization*, Macromolecules, **16**, 348-357 (1983).

Curteanu S., Bulacovschi V., *Modeling of Free Radical Polymerization of Styrene Using a Binary Mixture of Initiators and Isothermal Steps of Temperature*, Revue Roumaine de Chimie, **48**, *7*, 579-588 (2003).

Ding M., Wang J., Wu H., Zhou J., *Real-Time Correction of Molecular Weight Distribution Model Based on the Field-Measurable Moments*, IFAC-PapersOnLine, **48**, *28*, 933-938 (2015).

Hosen M.A., Hussain M.A., Mjalli F.S., *Control of Polystyrene Batch Reactors Using Neural Network Based Model Predictive Control (NNMPC): An Experimental Investigation*, Control Engineering Practice, **19**, 454-467 (2011).

Hosen M.A., Hussain M.A., *Optimization and Control of Polystyrene Batch Reactor Using Hybrid Based Model*, I.A. Karimi and Rajagopalan Srinivasan (Editors), Proceedings of the 11th International Symposium on Process Systems Engineering, 15-19 July 2012, Singapore. 2012 Elsevier B.V.

Hosen M.A., Khosravi A., Nahavandi S., Creighton D., *Prediction Interval-Based Neural Network Modelling of Polystyrene Polymerization Reactor – A New Perspective of Data-Based Modeling*, Chemical Engineering Research and Design, 92, 2041-2051 (2014).

MODELAREA POLIMERIZĂRII RADICALICE A STIRENULUI FOLOSIND REȚELE NEURONALE ARTIFICIALE

(Rezumat)

În această lucrare, modelarea polimerizării radicalice a stirenului se realizează utilizând două abordări: fenomenologică și empirică. În ultimul caz, se utilizează rețele neuronale artificiale, aplicând două strategii de lucru. În primul rând, a fost determinat un singur model cu trei ieșiri (conversia monomerului, mase moleculare numerice şi mase moleculare gravimetrice) pe baza timpului, temperaturii şi concentrației inițiale a inițiatorului. Datorită rezultatelor inacceptabile ale performanţelor pentru masele moleculare, se dezvoltă o a doua strategie, modelarea fiecărei ieșiri, separat, în funcție de cele trei intrări. Diferite topologii ale rețelelor neuronale artificiale au fost testate, rețeaua cu două straturi ascunse având cele mai bune rezultate.